and functional hippocampal deficits (Barnes, 1994; Geinisman et al., 1992).

Epigenetic changes involve transmissible alterations in gene expression caused by mechanisms other than changes in the DNA sequence. (Gravina and Vijg, 2009) Epigenetic information is destined to change during development and in the course of essential somatic functions. This makes it a more likely candidate for errors than its more stable DNA-sequence counterpart, changes in which have been well documented and increase during aging (Gravina and Vijg, 2009). Indeed, epegenomic alterations are now becoming increasingly recognized as part of aging and its associated pathologic phenotypes (Gravina and Vijg, 2009). To better understand such age-dependent epigenetic modification, in this study we focused on the decreased expression of doublecortin, which is frequently used as a marker of a migrated neuronal progenitor in the hippocampus of aged mice.

This study was conducted in accordance with the Guiding Principles for the Care and Use of Laboratory Animals, Hoshi University, as adopted by the Committee on Animal Research of Hoshi University, which is accredited by the Ministry of Education, Culture, Sports, Science and Technology of Japan. All efforts were made to minimize the number of animals used and their suffering.

Two- and from 24- to 28-month-old C57BL/6J mice were used in the present study. Animals were kept in a room with an ambient temperature of 23 ± 1°C and a 12-h light/dark cycle (lights on 8:00 AM to 8:00 PM). Food and water were available ad libitum.

Mice were deeply anesthetized with isoflurane (3%) and perfusion-fixed with 4% paraformaldehyde (pH 7.4). The brain was then removed quickly and the hippocampus was rapidly dissected and postfixed in 4% paraformaldehyde for 2 h. The hippocampus was permeated with 20% sucrose for 1 day and 30% sucrose for 2 days, and then frozen in an embedding compound (Sakura Finetechnical, Tokyo, Japan). All samples were stored at −30°C until use. The sections were cut transversely at a thickness of 8 μm on a cryostat (Leica CM1510, Leica Microsystems, Heidelberg, Germany). The hippocampus sections were blocked in 5% normal goat serum in 0.01 M phosphate-buffered saline (PBS) for 1 h at room temperature. Each primary antibody was diluted in 0.01 M PBS containing 5% normal goat serum (guinea pig polyclonal antibody to doublecortin [1:3500; Abcam Ltd., Cambridge, UK]), and incubated for two days overnight at 4°C. The samples were then rinsed and incubated with the appropriate secondary antibody conjugated with Alexa 488 for 2 h at room temperature. The slides were then coverslipped with PermaFluor Aqueous mounting medium (Immunon, Pittsburgh, PA). Fluorescence of immunolabeling was detected using a light microscope (Olympus AX-70; Olympus, Tokyo, Japan, and a Radiance 2000 laser-scanning microscope; BioRad, Richmond, CA), and photographed with a digital camera (Polaroid PDMCII/OL; Olympus).

Total RNA in the hippocampus of aged mice was extracted using the SV Total RNA Isolation system (Promega, Madison, WI) following the manufacturer's instructions. Purified total RNA was quantified spectrophotometrically at A_{260}. To prepare first-strand cDNA, 1 μg of RNA was incubated in 100 μl of buffer containing 10 mM dithiothreitol, 2.5 mM $MgCl_2$, dNTP mixture, 50 U of reverse transcriptase II (Invitrogen, Carlsbad, CA), and 0.1 mM oligo-$dT_{12\text{-}18}$ (Invitrogen). Each gene was amplified in 50 μl of PCR solution containing 0.8 mM $MgCl_2$, dNTP mixture, and DNA polymerase with synthesized primers (Table I). Samples were heated to 95°C for 1 min, 55°C for 2 min, and 72°C for 3 min. The final incubation was at 72°C for 7 min. The mixture was run on 2% agarose gel electrophoresis with the indicated markers and primers for the internal standard glyceraldehyde-3-phosphate dehydrogenase. The agarose gel was stained with ethidium bromide and photographed with UV transillumination. The intensity of the bands was analyzed and semiquantified by computer-assisted densitometry using ImageJ software. Values represent the mean ± SEM of three independent experiments.

TABLE I. Comprehensive List of All Primer Sequences Used

Experiment	Name	Sequence
RT-PCR	DCX	F: CTTTTGGTTCAGCAGAAGGG
		R: CAAATGTTCTGGGAGGCACT
	GFAP	F: ACAACTTTGCACAGGACCTC
		R: CGATTCAACCTTTCTCTCCA
	BDNF	F: TCACTGGCTGACACTTTTGAG
		R: CTATCCTTATGAATCGCCAGC
	MLL1	F: AGCGGAGAGGATGAGCAGT
		R: CGAGGTTTTCGAGGACTAGC
	LSD1	F: TCAACGTCCTCAATAATAAACCTGT
		R: CCTGAGTTTTCACTATCTTCTTCCA
	Jaridla	F: CCTCCATTTGCCTGTGAAGT
		R: CCTTTGCTGGCAACAATCTT
	Jaridlb	F: AGAGGCTGAATGAGCTGGAG
		R: TGGCAATTTTGGTCCATTTT
	jmjd2A	F: GACCACACTCTGCCCACAC
		R: TCCTGGGGTATTTCCAGACA
	jmjd2B	F: GGCTTTAACTGCGCTGAGTC
		R: GTGTGGTCCAGCACTGTGAG
	jmjd2C	F: CACGGAGGACATGGATCTCT
		R: CGAAGGGAATGCCATACTTC
	jmjd2D	F: GTCTTGGTCGTCGTCCTTGT
		R: AATCCCCCTTCAGAAGCTGT
	EZH2	F: GCCAGACTGGGAAGAAATCTG
		R: TGTGCTGGAAAATCCAAGTCA
	UTX	F: ATCCCAGCTCAGCAGAAGTT
		R: GGAGGAAAGAAAGCATCACG
	jmjd3	F: CCCCCATTTCAGCTGACTAA
		R: CTGGACCAAGGGGTGTGTT
	GAPDH	F: CCCCACGGCAAGTTCAACGG
		R: CTTTCCAGAGGGCCATCCA
Real-time PCR	DCX	F: CTTTTGGTTCAGCAGAAGGG
		R: CAAATGTTCTGGGAGGCACT
	β-actin	F: CAGCTTCTTTGCAGCTCCTT
		R: TCACCCACATAGGAGTCCTT
ChIP	DCX	F: AGCTTGCCTGTGCAATCTTT
		R: GAACACCCCCAACCTCCTAT

Fast SYBR Green Master Mix (2x) (Applied Biosystems, Inc., CA) was used as the basis for the reaction mixture in the real-time PCR assay. Each gene prepared by the above procedure was amplified in 20 μl of a PCR solution containing 10 μl of the Fast SYBR Green Master Mix (2x) with synthesized primers (Table I). In addition to each sample, each test run included a no-target control that contained reaction mixture and PCR-grade water. PCR with a StepOnePlus™ (Applied Biosystems, Inc., CA) was performed with the following cycling conditions: 95°C for 20 s, followed by 45 cycles of 95°C for 3 s and 60°C for 30 s. Fluorescence detection was conducted after each extension step.

A ChIP assay was performed as described previously (Takeshima et al., 2009; Tsankova et al., 2004) with minor modifications. Briefly, mouse hippocampus tissue was dissected as described above and cross-linked, and then tissue was lysed. Fifteen μg of soluble chromatin was incubated with 2 μg of specific antibodies against acetylated histone H3 (Millipore), H3K4 trimethylation (Wako Pure Chemicals, Osaka, Japan), H3K9 trimethylation (Millipore), H3K27 trimethylation (Millipore), overnight at 4°C. The immunocomplex was collected by Dynabeads Protein A (Invitrogen Dynal AS, Oslo, Norway), and DNA was recovered with RNaseA treatment, Proteinase K treatment followed by isopropanol precipitation. Immunoprecipitated DNA was dissolved in 50 μl of 1 × TE and 1 μl was used for quantitative PCR. Quantitative PCR was performed as described previously (Nakajima et al., 2009). The primers used are listed in Table I.

The data are expressed as the mean ± S.E.M. The statistical significance of differences between groups was assessed with Student's *t*-test (comparison of two groups) or an analysis of variance (ANOVA) followed by the Bonferroni test (comparison among multiple groups). A level of probability of 0.05 or less was considered significant.

Doublecortin is a cytoskeletal protein that is transiently expressed only in newborn neurons, and is used as a marker of neural progenitors. In agreement with a previous report (Hwang et al., 2008), we confirmed that doublecortin-positive cells were almost completely absent from the dentate gyrus of the hippocampus of 28-month-old mice (Fig. 1A). The level of doublecortin, the doublecortin mRNA was significantly decreased in the hippocampus of aged mice compared to that in young mice (Figs. 1B and 1C, $P < 0.001$ vs. young mice). In contrast, mRNA levels of glial fibrillary acidic protein (GFAP), a glial marker, and brain-derived neurotrophic factor (BDNF) in the hippocampus were not altered by normal aging.

We next evaluated whether changes in doublecortin mRNA expression accompanied by aging could be regulated through chromatin-specific events. In this study, we analyzed two active histone modifications (acetylation of histone H3, AcH3, and trimethylation of lysine 4 on histone H3, H3K4) and two repressive histone modifications (trimethylation of lysine 9 on histone H3, H3K9, and trimethylation of lysine 27 on histone H3, H3K27) at doublecortin promoter regions in the hippocampus. As a result, we detected a significant decrease in H3K4 trimethylation at the doublecortin promoters with aging (Fig. 2A, $P < 0.05$ vs. young mice). Furthermore, a significant increase in H3K27 trimethylation at the doublecortin gene was seen with aging (Fig. 2A, $P < 0.05$ vs. young mice). Under these conditions, aging did not produce H3K9 trimethylation or hyperacetylation of H3 at the doublecortin gene (Fig. 2A).

The methylation of H3K9 and H3K27 can be directly modulated by histone methylases and demethylases that target specific lysine residues and methylation states. Thus, we finally investigated whether aging could alter the mRNA level of several histone methylases and demethylases in the hippocampus. We found that aging did not change the mRNA expression of MLL1 (a H3K4 methyltransferase), LSD1, Jarid1a or Jarid1b (H3K4 demethylases), jmjd2A, jmjd2B, jmjd2C or jmjd2D (H3K9 demethylases), EZH2 (a H3K27 methyltransferase), or UTX or jmjd3 (H3K27 demethylases) (Fig. 2B).

Doublecortin is a microtubule-associated protein that is expressed specifically in virtually all migrating neural precursors of the CNS and has been used as a candidate marker for neuronal migration and differentiation. In this study, aging caused a dramatic decrease in levels of doublecortin mRNA in the hippocampus. In the dentate gyrus of the hippocampus, few or no doublecortin-positive cells were observed by aging. These findings strongly suggest that an aging can stimulate the impairment of neuronal differentiation from precursors in the hippocampal dentate gyrus. These notions are supported by previous reports that aging promoted the impairment of neurogenesis (Kuhn et al., 1996; Lichtenwalner et al., 2001).

Epigenetic alterations of DNA play key roles in determining gene structure and expression (Jaenisch and Bird, 2003; Tsankova et al., 2007). A major epigenetic modification, chromatin remodeling, modulates gene expression with high temporal and spatial resolution by permitting small groups of nucleosomes to become more or less open, which consequently enhances or inhibits access of the transcriptional machinery to specific promoter regions. The acetylation and methylation of histone proteins at specific residues play a major role in chromatin remodeling. Lysine acetylation almost always correlates with chromatin accessibility and transcriptional activity, whereas lysine methylation can have different effects depending on which residue is modified. Trimethylation of H3K4

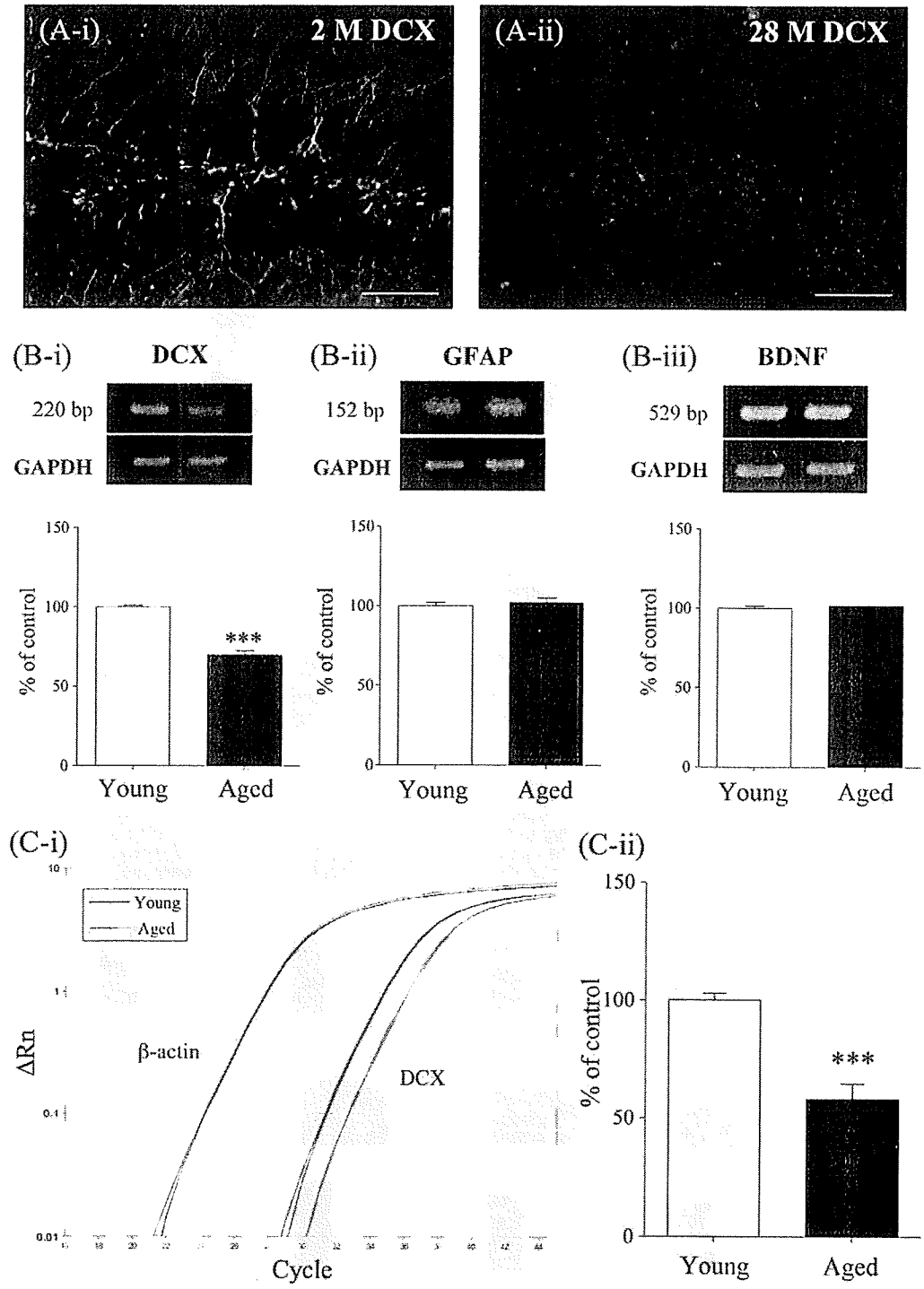

Fig. 1. (A) Immunofluorescent staining for doublecortin in the dentate gyrus in young and aged mice. Doublecortin-like immunoreactivity in the dentate gyrus of 28-month-old mice (A-ii) was decreased compared to that in 2-month-old mice (A-i). Scale bar: 50 μm. (B) Upper: Representative RT-PCR for doublecortin (DCX; B-i), GFAP (B-ii) and BDNF (B-iii) mRNAs in the hippocampus obtained from young and aged mice. Lower: The intensity of the bands was semiquantified using NIH Image software. The values for DCX, GFAP and BDNF mRNA were normalized by that for the internal standard glyceraldehyde-3-phosphate dehydrogenase (GAPDH) mRNA. The value for aged mice is expressed as a percentage of the increase in young mice. Each column represents the mean ± S.E.M. six samples. $^{***}P < 0.001$ vs. the young group. (C) Quantitative analysis of DCX mRNA in the hippocampus obtained from young and aged mice. (C-i) Amplification plots of fluorescence intensities vs. PCR cycle numbers in each sample. (C-ii) Each column represents the mean ± S.E.M. of three samples. $^{***}P < 0.001$ vs. the young group.

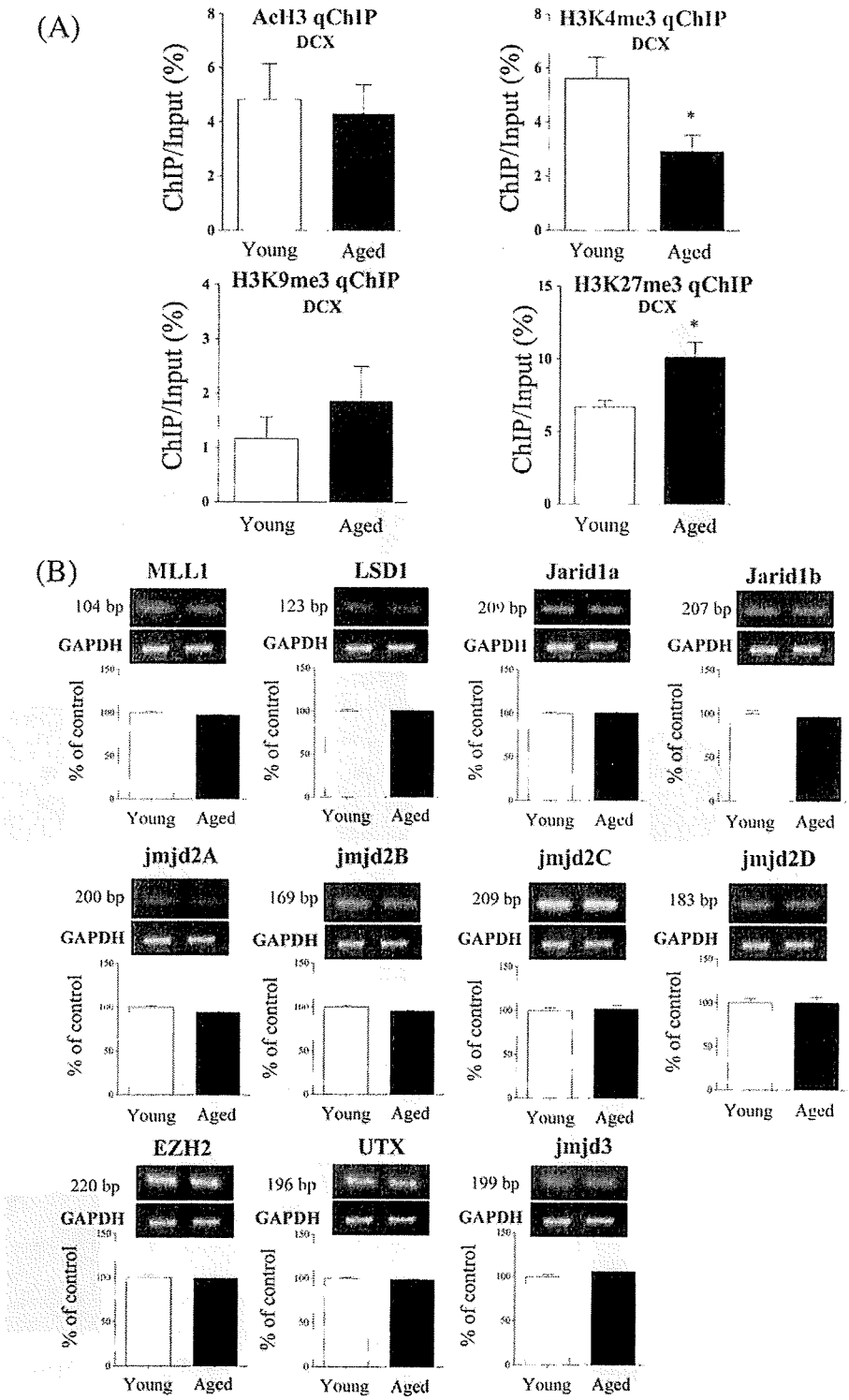

Fig. 2. **A**: Stable changes in histone modifications in the hippocampus in aged mice. ChIP assays were performed to measure the levels of several histone modifications at the doublecortin (DCX) promoter in the hippocampus using specific antibodies for each modification state. Levels of promoter enrichment were quantified by quantitative PCR. Histone H3 was not altered at DCX. Significant changes in acetylation (AcH3) or H3K9 trimethylation (H3K9me3) were not detected at the DCX promoter region. Histone H3K4 trimethylation (H3K4me3) was decreased at the DCX promoter region in aged mice. $^*P < 0.05$ vs. the young group. Histone H3K27 trimethylation (H3K27me3) was increased at the DCX promoter region in aged mice. $^*P < 0.05$ vs. the young group. **B**: Upper: Representative RT-PCR for MLL1 (a H3K4 methyltransferase), LSD1, Jarid1a and Jarid1b (H3K4 demethylases), jmjd2A, jmjd2B, jmjd2C and jmjd2D (H3K9 demethylases), and EZH2 (a H3K27 methyltransferase), and UTX and jmjd3 (H3K27 demethylases). mRNAs in the hippocampus obtained from young and aged mice. Lower: The intensity of the bands was semiquantified using NIH Image software. The value for mRNA was normalized by that for the internal standard glyceraldehyde-3-phosphate dehydrogenase (GAPDH) mRNA. The value for aged mice is expressed as a percentage of the increase in young mice. Each column represents the mean ± S.E.M. of six samples.

is associated with transcribed chromatin. In contrast, trimethylation of H3K9 and H3K27 generally correlates with repression (Bernstein et al., 2007). In agreement with the PCR assay, we found here that aging caused a significant decrease in H3K4 trimethylation and a significant increase in H3K27 trimethylation at the doublecortin gene. In contrast, we failed to find any changes in the H3K9 trimethylation and hyperacetylation of H3 at the doublecortin gene. These findings suggest that aging produces a dramatic decrease in the expression of the neuronal progenitor doublecortin along with epigenetic modifications in the hippocampus.

Histone methylation is dynamically regulated by a plethora of methylases and demethylases (Swigut and Wysocka, 2007). In the present study, aging failed to change the mRNA expression of several methylases and demethylases including MLL1 (a H3K4 methyltransferase), LSD1, Jarid1a and Jarid1b (H3K4 demethylases), jmjd2A, jmjd2B, jmjd2C and jmjd2D (H3K9 demethylases), EZH2 (a H3K27 methyltransferase), and UTX and jmjd3 (H3K27 demethylases). These findings suggest that aging causes a dramatic decrease in neurogenesis accompanied by epigenetic modification related to the decreased expression of doublecortin without changing the expression of their associated histone methylases and demethylases in the hippocampus.

In conclusion, although further investigation is still required, the present findings suggest that decreased expression of the migrated neural progenitor doublecortin associated with histone modification may be, at least in part, involved in an aging-dependent decrease in neurogenesis in the hippocampus. Since the methylation of H3K27 is especially considered to play a critical role in the long-lasting silencing of targeted gene expression (Swigut and Wysocka, 2007), the present finding of the epigenetically repressive modulation of neural progenitors could allow us to better understand the mechanism of aging-dependent hippocampal dysfunction.

REFERENCES

Barnes CA. 1994. Normal aging: Regionally specific changes in hippocampal synaptic transmission. Trends Neurosci 17:13–18.

Bernstein BE, Meissner A, Lander ES. 2007. The mammalian epigenome. Cell 128:669–681.

Bliss TV, Collingridge GL. 1993. A synaptic model of memory: Long-term potentiation in the hippocampus. Nature 361:31–39.

Eriksson PS, Perfilieva E, Bjork-Eriksson T, Alborn AM, Nordborg C, Peterson DA, Gage FH. 1998. Neurogenesis in the adult human hippocampus. Nat Med 4:1313–1317.

Geinisman Y, DeToledo-Morrell L, Morrell F, Persina IS, Rossi M. 1992. Age-related loss of axospinous synapses formed by two afferent systems in the rat dentate gyrus as revealed by the unbiased stereological dissector technique. Hippocampus 2:437–444.

Gravina S, Vijg J. 2009. Epigenetic factors in aging and longevity. Pflugers Arch (in press).

Hwang IK, Yoo KY, Yi SS, Kwon YG, Ahn YK, Seong JK, Lee IS, Yoon YS, Won MH. 2008. Age-related differentiation in newly generated DCX immunoreactive neurons in the subgranular zone of the gerbil dentate gyrus. Neurochem Res 33:867–872.

Jaenisch R, Bird A. 2003. Epigenetic regulation of gene expression: How the genome integrates intrinsic and environmental signals. Nat Genet 33 (Suppl):245–254.

Kempermann G, Kuhn HG, Gage FH. 1997. More hippocampal neurons in adult mice living in an enriched environment. Nature 386: 493–495.

Kuhn HG, Dickinson-Anson H, Gage FH. 1996. Neurogenesis in the dentate gyrus of the adult rat: Age-related decrease of neuronal progenitor proliferation. J Neurosci 16:2027–2033.

Lichtenwalner RJ, Forbes ME, Bennett SA, Lynch CD, Sonntag WE, Riddle DR. 2001. Intracerebroventricular infusion of insulin-like growth factor-I ameliorates the age-related decline in hippocampal neurogenesis. Neuroscience 107:603–613.

Lois C, Alvarez-Buylla A. 1993. Proliferating subventricular zone cells in the adult mammalian forebrain can differentiate into neurons and glia. Proc Natl Acad Sci USA 90:2074–2077.

Nakajima T, Yamashita S, Maekita T, Niwa T, Nakazawa K, Ushijima T. 2009. The presence of a methylation fingerprint of *Helicobacter pylori* infection in human gastric mucosae. Int J Cancer 124:905–910.

Swigut T, Wysocka J. 2007. H3K27 demethylases, at long last. Cell 131:29–32.

Takeshima H, Yamashita S, Shimazu T, Niwa T, Ushijima T. 2009. The presence of RNA polymerase II, active or stalled, predicts epigenetic fate of promoter CpG islands. Genome Res 19:1974–1982.

Tsankova NM, Kumar A, Nestler EJ. 2004. Histone modifications at gene promoter regions in rat hippocampus after acute and chronic electroconvulsive seizures. J Neurosci 24:5603–5610.

Tsankova N, Renthal W, Kumar A, Nestler EJ. 2007. Epigenetic regulation in psychiatric disorders. Nat Rev Neurosci 8:355–367.

van Praag H, Kempermann G, Gage FH. 1999. Running increases cell proliferation and neurogenesis in the adult mouse dentate gyrus. Nat Neurosci 2:266–270.

RAPID COMMUNICATION

Hippocampal Epigenetic Modification at the Brain-Derived Neurotrophic Factor Gene Induced by an Enriched Environment

Naoko Kuzumaki,[1] Daigo Ikegami,[1] Rie Tamura,[1] Nana Hareyama,[1] Satoshi Imai,[1] Michiko Narita,[1] Kazuhiro Torigoe,[1] Keiichi Niikura,[1] Hideyuki Takeshima,[2] Takayuki Ando,[2] Katsuhide Igarashi,[3] Jun Kanno,[3] Toshikazu Ushijima,[2] Tsutomu Suzuki,[1*] and Minoru Narita[1*]

ABSTRACT: Environmental enrichment is an experimental paradigm that increases brain-derived neurotrophic factor (BDNF) gene expression accompanied by neurogenesis in the hippocampus of rodents. In the present study, we investigated whether an enriched environment could cause epigenetic modification at the BDNF gene in the hippocampus of mice. Exposure to an enriched environment for 3–4 weeks caused a dramatic increase in the mRNA expression of BDNF, but not platelet-derived growth factor A (PDGF-A), PDGF-B, vascular endothelial growth factor (VEGF), nerve growth factor (NGF), epidermal growth factor (EGF), or glial fibrillary acidic protein (GFAP), in the hippocampus of mice. Under these conditions, exposure to an enriched environment induced a significant increase in histone H3 lysine 4 (H3K4) trimethylation at the BDNF P3 and P6 promoters, in contrast to significant decreases in histone H3 lysine 9 (H3K9) trimethylation at the BDNF P4 promoter and histone H3 lysine 27 (H3K27) trimethylation at the BDNF P3 and P4 promoters without any changes in the expression of their associated histone methylases and demethylases in the hippocampus. The expression levels of several microRNAs in the hippocampus were not changed by an enriched environment. These results suggest that an enriched environment increases BDNF mRNA expression via sustained epigenetic modification in the mouse hippocampus. © 2010 Wiley-Liss, Inc.

KEY WORDS: mouse hippocampus; epigenome; BDNF gene; neurogenesis; environmental enrichment

INTRODUCTION

Over the past few decades, exposure to an enriched environment, which consists of housing groups of animals together in a complex environment with various toys to provide more opportunity for learning and social interaction than standard laboratory living conditions, has been shown to enhance behavioral performance in various learning tasks. Consistent with these behavioral tests, exposure to an enriched environment has been shown to induce biochemical and structural changes in the hippocampal dentate gyrus (DG) and CA1 region, such as an increased number of dendritic branches and spines, enlargement of synapses, and an increased number of glial cells. Moreover, exposure of adult rodents to increased environmental complexity induces hippocampal progenitor proliferation and neurogenesis (Nilsson et al., 1999; van Praag et al., 1999). However, the detailed mechanisms that control neurogenesis in the hippocampus of animals housed in an enriched environment are still unclear.

It has been reported that brain-derived neurotrophic factor (BDNF) promotes neuronal differentiation from endogenous progenitor cells in the ventricular wall of the adult forebrain (Ahmed et al., 1995; Kirschenbaum and Goldman, 1995), and the increased expression of BDNF is required for the environmental induction of hippocampal neurogenesis in rodents (Rossi et al., 2006). The BDNF gene and the regulation of its expression are highly complex, and have been examined in both human and rodent brains (Timmusk et al., 1993; Liu et al., 2006; Aid et al., 2007; Pruunsild et al., 2007). The mouse BDNF gene, which shows a high degree of sequence homology to its human congener, contains multiple 5′ noncoding exons and a single 3′ coding exon for the mature BDNF protein (Aid et al., 2007). These noncoding exons undergo alternative splicing with the common coding exon to produce multiple exon-specific BDNF transcripts. Nine BDNF promoters have been previously identified in the mouse (Aid et al., 2007), and each drives the transcription of BDNF mRNAs containing one of the four 5′ noncoding exons (I, II, III, IV, V, VI, VII, or VIII) spliced to the common 3′ coding exon.

[1] Department of Toxicology, Hoshi University School of Pharmacy and Pharmaceutical Sciences, 2-4-41 Ebara, Shinagawa-ku, Tokyo 142-8501, Japan; [2] Carcinogenesis Division, National Cancer Center Research Institute, 5-1-1 Tsukiji, Chuo-ku, Tokyo 104-0045, Japan; [3] Division of Cellular and Molecular Toxicology, Biological Safety Research Center, National Institute of Health Sciences, 1-18-1, Kamiyoga, Setagaya-ku, Tokyo 154-0000, Japan

Additional Supporting Information may be found in the online version of this article.

Grant sponsor: Ministry of Education, Culture, Sports, Science and Technology of Japan

*Correspondence to: Minoru Narita, Ph.D., Department of Toxicology, Hoshi University School of Pharmacy and Pharmaceutical Sciences, 2-4-41 Ebara, Shinagawa-ku, Tokyo 142-8501, Japan. E-mail: narita@hoshi.ac.jp and Tsutomu Suzuki, Ph.D., Department of Toxicology, Hoshi University School of Pharmacy and Pharmaceutical Sciences, 2-4-41 Ebara, Shinagawa-ku, Tokyo 142-8501, Japan. E-mail: suzuki@hoshi.ac.jp

Accepted for publication 22 December 2009
DOI 10.1002/hipo.20775
Published online in Wiley InterScience (www.interscience.wiley.com).

Chromatin remodeling at gene promoter regions is becoming increasingly recognized as a key control point of gene expression. Histone modification represents one prominent form of chromatin remodeling. According to the "histone code theory," different modifications of histones at a particular promoter region, alone or in combination, define a specific epigenetic state that encodes gene activation vs. gene silencing (Jenuwein and Allis, 2001). Intriguing correlations have been found between cellular plasticity, including transformation and such epigenetic modification at a specific gene (Kouzarides, 2007; Borrelli et al., 2008), indicating that possible epigenetic modification at BDNF gene promoters may partly contribute to adult neurogenesis. Therefore, in the present study, we evaluated whether an enriched environment could induce histone modification at several BDNF gene promoters in mice.

Male C57BL/6J mice (Jackson Laboratory), weighing 18–23 g, were used in the present study. Control mice were housed four per standard (16.5 × 26.5 × 13.5 cm^3) plexiglass cage. Mice

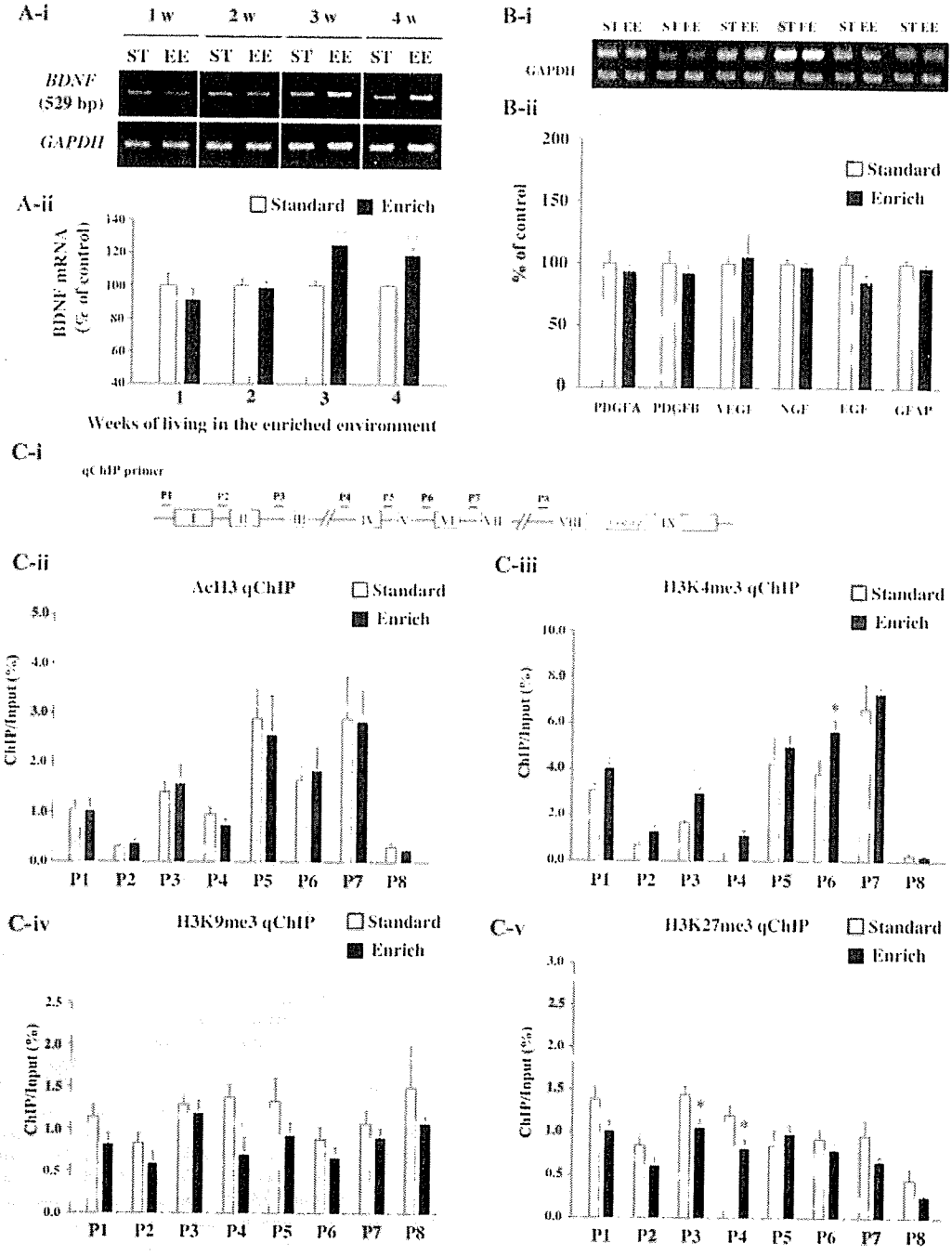

in the enriched environment group were kept eight per large (25.5 × 42.5 × 39 cm^3) wire-mesh, two-storied cage, which contained tunnels and running wheels, for 4 weeks (Supporting Information Fig. 1A).

In the DG of mice housed in the enriched environment for 4 weeks, immunoreactivity (IR) for doublecortin, which is a microtubule-associated protein that is expressed specifically in virtually all migrating neuronal precursors of the CNS and which has been used as a candidate marker for neural migration and differentiation, was increased compared to that in mice housed in the standard cage (Supporting Information Fig. 1B). Furthermore, IR for NeuroD, which is another marker for the differentiation of granule cells in the hippocampus (Miyata et al., 1999), was clearly increased in the DG of mice housed in an enriched environment (Supporting Information Fig. 1C). Additionally, the number of BrdU-positive cells in the DG that were classified as newly dividing cells was markedly increased in mice housed in an enriched environment (Supporting Information Fig. 2A), and theses were clearly colocalized with the neuronal marker NeuN (Supporting Information Fig. 2B). In paralleled with adult neurogenesis, the expression of BDNF mRNA in the hippocampus was significantly elevated after exposure to an enriched environment for both 3 and 4 weeks (Fig. 1A). In contrast, mRNA levels of glial fibrillary acidic protein (GFAP), platelet-derived growth factor A (PDGF-A), PDGF-B, vascular endothelial growth factor (VEGF), nerve growth factor (NGF), and epidermal growth factor (EGF) in the hippocampus were not altered by exposure to an enriched environment for 4 weeks (Fig. 1B).

Under these conditions, a significant increase in histone H3 lysine 4 (H3K4) trimethylation at the BDNF P3 and P6 promoters was observed upon exposure to an enriched environment for 4 weeks. Furthermore, significant decreases in histone H3 lysine 9 (H3K9) trimethylation at the BDNF P4 promoter, and histone H3 lysine 27 (H3K27) trimethylation at the BDNF P3 and P4 promoters were seen in the hippocampus of mice under an enriched environment. In contrast, an enriched environment did not produce the hyperacetylation of H3 in the hippocampus of enriched mice (Fig. 1C).

In terms of changes in mRNA levels of several histone methylases and demethylases in the hippocampus, an enriched environment failed to change the mRNA expression of MLL1, LSD1, Jarid1a, Jarid1b, jmjd2B, jmjd2C, jmjd2D, EZH2, UTX, or jmjd3 (Fig. 2A).

As with histone methylases and demethylases, no significant changes in microRNA9 (miR9), miR124a, miR132, miR133b, or miR145 were observed in the hippocampus of mice housed in an enriched environment for 2 and 4 weeks compared to mice housed in a standard cage (Fig. 2B).

In the present study, we demonstrated hippocampal neurogenesis in mice that were exposed to an enriched environment. This notion is supported by previous reports that exposure of adult rodents to an enriched environment increased neurogenesis in the hippocampus (Kempermann et al., 1997; Nilsson et al., 1999).

During development, growth factors provide important extracellular signals that regulate the proliferation and differentiation of neural stem cells in the CNS (Calof, 1995). Several investigations have examined the role of these factors in the adult brain (Calof, 1995; Kuhn et al., 1997). Furthermore, it has been shown that exposure to an enriched environment increased the expression of BDNF genes (Falkenberg et al., 1992). In support of these findings, the present study showed that the expression of BDNF mRNA in the hippocampus was significantly elevated after exposure to an enriched environment for both 3 and 4 weeks. In contrast, mRNA levels of GFAP, PDGF-A, PDGF-B, VEGF, NGF, and EGF in the hippocampus were not altered under the present conditions. In our *in vitro* study using neural stem cells cultured from the mouse embryonic forebrain, neuronal differentiation was clearly observed following exposure to recombinant BDNF (Supporting Information Fig. 3). These findings raise the possibility that an enriched environment may stimulate expression of the BDNF gene in the hippocampus and, in turn, the enhanced

FIGURE 1. **(A) Time course of changes in the expression of BDNF mRNA in the hippocampus. (A-i) Representative RT-PCR for BDNF mRNA in the hippocampus obtained from standard or enriched mice. (A-ii) The intensity of the bands was semiquantified using NIH Image software. The value for BDNF mRNA was normalized by that for the internal standard glyceraldehyde-3-phosphate dehydrogenase (GAPDH) mRNA. The value for enriched mice is expressed as a percentage of the increase in standard mice. Each column represents the mean ± S.E.M. of six samples. **$P < 0.01$ vs. the standard group. (B) Upper: Representative RT-PCR for PDGFA, PDGFB, VEGF, NGF, EGF, and GFAP mRNAs in the hippocampus obtained from standard or enriched mice. Lower: The values for mRNAs were normalized by that for GAPDH mRNA. Each column represents the mean ± S.E.M. of six samples. (C-i) Schematic of the BDNF gene: The BDNF gene contains eight noncoding exons I–VIII upstream of the coding exon IX in mouse. Exons I–VIII can each be alternatively spliced next to exon IX, from the 5′ UTR region of different mRNA splice variants, BDNF I-VIII, which can promote the expression of their corresponding transcript variants. For an mRNA analysis of total BDNF, primers were used to amplify exon IX. For ChIP analysis, primers were designed around the putative promoters, P1-P8, which are located upstream of exons I–VIII. (C-ii, iii, iv, v) Stable changes in histone modifications in the hippocampus in mice housed under standard or enriched conditions for 4 weeks. ChIP assays were performed to measure the levels of several histone modifications at the eight BDNF promoters Ex1-Ex8 (P1–8) in the hippocampus using specific antibodies for each modification state. Levels of promoter enrichment were quantified by quantitative PCR. (C-ii) Histone H3 was not altered at BDNF P1–P8. (C-iii) Histone H3K4 trimethylation was increased at BDNF P3 and P6 in mice housed under enriched conditions for 4 weeks. *$P < 0.05$ vs. the standard group, **$P < 0.01$ vs. the standard group. (C-iv) H3K9 trimethylation was decreased at BDNF P4 in mice housed under enriched conditions for 4 weeks. *$P < 0.05$ vs. the standard group. (C-v) Histone H3K27 trimethylation was decreased at BDNF P3 and P4 in mice housed under enriched conditions for 4 weeks. *$P < 0.05$ vs. the standard group.**

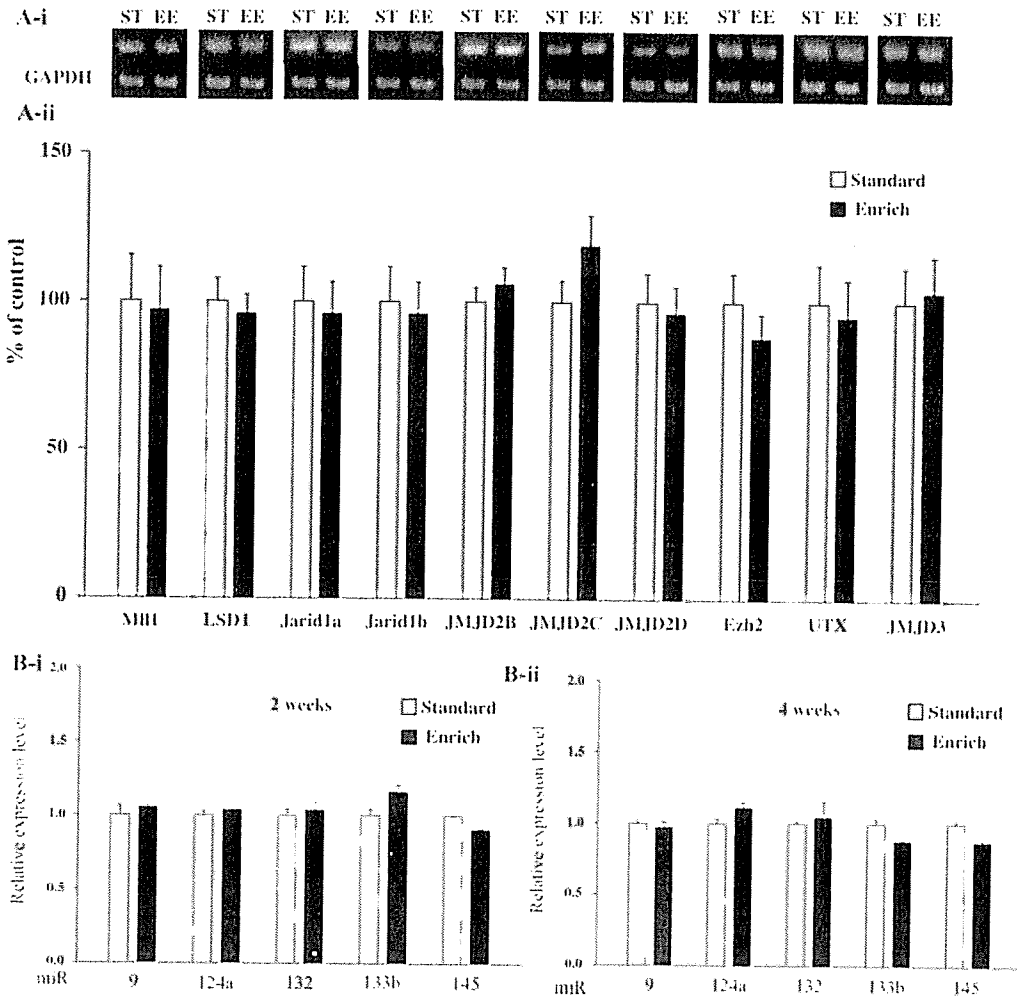

FIGURE 2. (A) Upper: Representative RT-PCR for MLL1 (an H3K4 methyltransferase), LSD1, Jarid1a, and Jarid1b (H3K4 demethylases), JMJD2B, JMJD2C and JMJD2D (H3K9 demethylases), Ezh2 (H3K27 methyltransferase), and UTX and JMJD3 (H3K27 demethylases). mRNAs in the hippocampus obtained from standard or enriched mice. Lower: The value for mRNA was normalized by that for GAPDH mRNA. Each column represents the mean ± SEM of six samples. (B) Expression levels of miRNAs were measured in the hippocampus of mice housed in an enriched environment for 2 weeks (B-i) and 4 weeks (B-ii). The value for miRNA was normalized by that for the internal standard snoRNA202.

BDNF protein may lead to neural differentiation from its precursors in the hippocampal DG.

We next evaluated whether an enriched environment increases BDNF gene expression through chromatin-specific events that promote the expression of distinct transcript variants. In this study we analyzed two active histone modifications (acetylation of histone H3, AcH3, and trimethylation of H3K4) and two repressive histone modifications (trimethylation of H3K9 and trimethylation of H3K27) at different BDNF promoter regions in the hippocampus. As a result, we detected a significant increase in H3K4 trimethylation, an activated histone modification marker, at the BDNF P3 and P6 promoters after exposure to an enriched environment for 4 weeks. Furthermore, significant decreases in H3K9 trimethylation, a repressive histone modification marker, at the BDNF P4 promoter, and H3K27 trimethylation, another repressive histone modification marker, at the BDNF P3 and P4 promoters were seen after exposure to an enriched environment. Under these conditions, we observed that an enriched environment did not produce the hyperacetylation of H3 in enriched mice.

The methylation of H3K9 and H3K27 can be directly modulated by histone methylases and demethylases that target specific lysine residues and methylation states (Jenuwein and Allis, 2001; Kouzarides, 2007). Thus, we investigated whether an enriched environment could alter the mRNA level of several histone methylases and demethylases in the hippocampus. We found that an enriched environment did not change the

mRNA expression of MLL1 (an H3K4 methyltransferase), LSD1, Jarid1a or Jarid1b (H3K4 demethylases), jmjd2B, jmjd2C or jmjd2D (H3K9 demethylases), EZH2 (an H3K27 methyltransferase), or UTX or jmjd3 (H3K27 demethylases).

Recently, microRNAs (miRNAs), a class of small, noncoding RNAs, have been identified as important regulators of many biological processes, including organogenesis and disease development (Kim et al., 2007; Chen et al., 2008; Hutchison et al., 2009). Indeed, it has been shown that epigenetic factors such as DNA methylation, histone modification, and regulatory noncoding RNAs affect the fate of neural stem cells (Chi and Bernstein, 2009). miRNAs have the potential to specifically regulate a large set of target molecules, which may affect the cell's fate in a programmatic way, and the role of miRNAs in stem cell gene networks is being actively explored. Their ability to potentially regulate large numbers of target genes simultaneously suggests that they may be important sculptors of transcriptional networks. In this study, we found that miR9, miR124a, miR132, miR133b, and miR145 are expressed in the hippocampus of adult mice. It has been reported that miR145 regulates Oct4, Sox2, and Klf4 and suppresses the potential of human embryonic stem cells to generate any differentiated cell type (pluripotency) (Xu et al., 2009). miR124, one of these signature miRNAs that is enriched in the brain, regulates adult neurogenesis in the subventricular zone stem cell niche (Cheng et al., 2009). miR132 is localized and synthesized, in part, at synaptic sites in dendrites to regulate synaptic formation and plasticity (Vo et al., 2005). miR9 is expressed specifically in the hippocampus and may be involved in neural stem cell self-renewal and differentiation (Krichevsky et al., 2006; Bak et al., 2008). In the present study, there were no significant changes in miR9, miR124a, miR132, miR133b, or miR145 in the hippocampus of mice housed in an enriched environment for 2 and 4 weeks compared to mice housed in a standard cage. Although further studies are required to investigate the molecular mechanism of hippocampal neurogenesis induced by an enriched environment, we propose that an enriched environment may increase BDNF expression accompanied by histone modification without directly changing the expression of histone H3 methylases and demethylases, and miRs in the hippocampus.

In conclusion, the present study demonstrated that an enriched environment stimulates neuronal differentiation from precursors in the hippocampal DG. Furthermore, the increased expression of BDNF was observed in the hippocampus of mice that had been exposed to an enriched environment. This enrichment induced a significant increase in H3K4 trimethylation at the BDNF P3 and P6 promoters and a significant decrease in H3K9 trimethylation at the BDNF P4 promoter and H3K27 trimethylation at the BDNF P3 and P4 promoters in the hippocampus of mice. These results suggest that an enriched environment may increase BDNF expression with notably sustained chromatin regulation in the mouse hippocampus. This phenomenon could partly explain the hippocampal neurogenesis induced by an enriched environment in mice.

Acknowledgment

The authors thank Dr. Kazuya Miyagawa for their expert technical assistance.

REFERENCES

Ahmed S, Reynolds BA, Weiss S. 1995. BDNF enhances the differentiation but not the survival of CNS stem cell-derived neuronal precursors. J Neurosci 15:5765–5778.

Aid T, Kazantseva A, Piirsoo M, Palm K, Timmusk T. 2007. Mouse and rat BDNF gene structure and expression revisited. J Neurosci Res 85:525–535.

Bak M, Silahtaroglu A, Moller M, Christensen M, Rath MF, Skryabin B, Tommerup N, Kauppinen S. 2008. MicroRNA expression in the adult mouse central nervous system. RNA 14:432–444.

Borrelli E, Nestler EJ, Allis CD, Sassone-Corsi P. 2008. Decoding the epigenetic language of neuronal plasticity. Neuron 60:961–974.

Calof AL. 1995. Intrinsic and extrinsic factors regulating vertebrate neurogenesis. Curr Opin Neurobiol 5:19–27.

Chen X, Zhang J, Fang Y, Zhao C, Zhu Y. 2008. Ginsenoside Rg1 delays tert-butyl hydroperoxide-induced premature senescence in human WI-38 diploid fibroblast cells. J Gerontol A Biol Sci Med Sci 63:253–264.

Cheng LC, Pastrana E, Tavazoie M, Doetsch F. 2009. miR-124 regulates adult neurogenesis in the subventricular zone stem cell niche. Nat Neurosci 12:399–408.

Chi AS, Bernstein BE. 2009. Developmental biology. Pluripotent chromatin state. Science 323:220–221.

Falkenberg T, Mohammed AK, Henriksson B, Persson H, Winblad B, Lindefors N. 1992. Increased expression of brain-derived neurotrophic factor mRNA in rat hippocampus is associated with improved spatial memory and enriched environment. Neurosci Lett 138:153–156.

Hutchison ER, Okun E, Mattson MP. 2009. The therapeutic potential of microRNAs in nervous system damage, degeneration, and repair. Neuromolecular Med 11:153–161.

Jenuwein T, Allis CD. 2001. Translating the histone code. Science 293:1074–1080.

Kempermann G, Kuhn HG, Gage FH. 1997. More hippocampal neurons in adult mice living in an enriched environment. Nature 386:493–495.

Kim J, Inoue K, Ishii J, Vanti WB, Voronov SV, Murchison E, Hannon G, Abeliovich A. 2007. A MicroRNA feedback circuit in midbrain dopamine neurons. Science 317:1220–1224.

Kirschenbaum B, Goldman SA. 1995. Brain-derived neurotrophic factor promotes the survival of neurons arising from the adult rat forebrain subependymal zone. Proc Natl Acad Sci USA 92:210–214.

Kouzarides T. 2007. Chromatin modifications and their function. Cell 128:693–705.

Krichevsky AM, Sonntag KC, Isacson O, Kosik KS. 2006. Specific microRNAs modulate embryonic stem cell-derived neurogenesis. Stem Cells 24:857–864.

Kuhn HG, Winkler J, Kempermann G, Thal LJ, Gage FH. 1997. Epidermal growth factor and fibroblast growth factor-2 have different effects on neural progenitors in the adult rat brain. J Neurosci 17:5820–5829.

Liu QR, Lu L, Zhu XG, Gong JP, Shaham Y, Uhl GR. 2006. Rodent BDNF genes, novel promoters, novel splice variants, and regulation by cocaine. Brain Res 1067:1–12.

Miyata T, Maeda T, Lee JE. 1999. NeuroD is required for differentiation of the granule cells in the cerebellum and hippocampus. Genes Dev 13:1647–1652.

Nilsson M, Perfilieva E, Johansson U, Orwar O, Eriksson PS. 1999. Enriched environment increases neurogenesis in the adult rat dentate gyrus and improves spatial memory. J Neurobiol 39:569–578.

Pruunsild P, Kazantseva A, Aid T, Palm K, Timmusk T. 2007. Dissecting the human BDNF locus: Bidirectional transcription, complex splicing, and multiple promoters. Genomics 90:397–406.

Rossi C, Angelucci A, Costantin L, Braschi C, Mazzantini M, Babbini F, Fabbri ME, Tessarollo L, Maffei L, Berardi N, Caleo M. 2006. Brain-derived neurotrophic factor (BDNF) is required for the enhancement of hippocampal neurogenesis following environmental enrichment. Eur J Neurosci 24:1850–1856.

Timmusk T, Palm K, Metsis M, Reintam T, Paalme V, Saarma M, Persson H. 1993. Multiple promoters direct tissue-specific expression of the rat BDNF gene. Neuron 10:475–489.

van Praag H, Kempermann G, Gage FH. 1999. Running increases cell proliferation and neurogenesis in the adult mouse dentate gyrus. Nat Neurosci 2:266–270.

Vo N, Klein ME, Varlamova O, Keller DM, Yamamoto T, Goodman RH, Impey S. 2005. A cAMP-response element binding protein-induced microRNA regulates neuronal morphogenesis. Proc Natl Acad Sci USA 102:16426–16431.

Xu N, Papagiannakopoulos T, Pan G, Thomson JA, Kosik KS. 2009. MicroRNA-145 regulates OCT4, SOX2, and KLF4 and represses pluripotency in human embryonic stem cells. Cell 137:647–658.

International Immunopharmacology 10 (2010) 393–397

Contents lists available at ScienceDirect

International Immunopharmacology

journal homepage: www.elsevier.com/locate/intimp

Effects of tetrabromobisphenol A, a brominated flame retardant, on the immune response to respiratory syncytial virus infection in mice

Wataru Watanabe [a], Tomomi Shimizu [b], Rie Sawamura [b], Akane Hino [b], Katsuhiko Konno [c], Akihiko Hirose [d], Masahiko Kurokawa [b,*]

[a] Department of Microbiology, School of Pharmaceutical Sciences, Kyushu University of Health and Welfare, Yoshino 1714-1, Nobeoka, Miyazaki 882-8508, Japan
[b] Department of Biochemistry, School of Pharmaceutical Sciences, Kyushu University of Health and Welfare, Yoshino 1714-1, Nobeoka, Miyazaki 882-8508, Japan
[c] Department of Clinically Veterinary Medicine, School of Pharmaceutical Sciences, Kyushu University of Health and Welfare, Yoshino 1714-1, Nobeoka, Miyazaki 882-8508, Japan
[d] Division of Risk Assessment, Biological Safety Research Center, National Institute of Health Sciences, 1-18-1, Kamiyoga, Setagaya-ku, Tokyo 158-8501, Japan

ARTICLE INFO

Article history:
Received 1 December 2009
Accepted 28 December 2009

Keywords:
Respiratory syncytial virus
Tetrabromobisphenol A
Pneumonia
Cytokines
Double-positive CD4+CD8+ cells

ABSTRACT

Effects of the brominated flame retardants (BFRs), decabrominated diphenyl ether (DBDE), hexabromocyclododecane (HBCD), and tetrabromobisphenol A (TBBPA), on host immunity of mice were evaluated using respiratory syncytial virus (RSV) infection. Five-week-old female mice were fed a diet containing 1% BFRs for 28 days, and subsequently infected with RSV. No toxicological sign was observed in BFR-treated mice before infection. TBBPA significantly increased the pulmonary viral titer in the infected mice on day 5 post-infection, but DBDE and HBCD did not. Slight histological changes were observed in lung tissues of TBBPA-treated mice with mock infection. These changes due to TBBPA were much exacerbated by RSV infection. Cytokine analysis of bronchoalveolar lavage fluid (BALF) from RSV-infected mice treated with or without TBBPA revealed that TBBPA significantly increased the levels of tumor necrosis factor (TNF)-α, interleukin (IL)-6 and interferon (IFN)-γ at each time point after virus infection, but no change was observed for IL-1β and IL-12. The levels of IL-4 and IL-10, Th2 cytokines, significantly decreased. Thus, TBBPA caused unusual production of the various cytokines in RSV-infected mice. Flow cytometry revealed that the percentage of double-positive CD4+CD8+ cells, immature T lymphocytes, in the cell populations in BALF from RSV-infected mice increased due to TBBPA treatment. The change was not observed in spleen cells of TBBPA-treated mice. The response to RSV infection verified that TBBPA treatment affected the host immunity of mice. Irregular changes in cytokine production and immune cell populations due to TBBPA treatment were suggested to cause exacerbation of pneumonia in RSV-infected mice.

1. Introduction

Human respiratory syncytial virus (RSV), a member of the family *Paramyxoviridae*, is the most prevalent infectious agent of acute lower respiratory illness in infants and young children [1]. Infection and reinfection with RSV are frequent during the first few years of life, and most children are infected by 24 months of age [2]. Clinically severe RSV infection is seen primarily in young children with naïve immune systems and/or genetic predispositions [3], patients with suppressed T-cell immunity [1], and the elderly [4]. A murine model of RSV infection has been used to develop anti-viral drugs and vaccines [5]. In this murine model, the development of pneumonia reflects the severity of RSV infection, and the pneumonia is histopathologically similar to that in humans [6,7]. We previously demonstrated that the severity of the RSV infection significantly reflected the host immune condition [8]. This RSV infection mouse model was shown to be useful to evaluate the immunotoxicity of chemical compounds [9].

Recently, it was reported that long-term exposure to industrial compounds containing brominated flame retardants (BFRs) may be toxic to humans, especially infants and children [10]. There are five major BFRs, tetrabromobisphenol A (TBBPA), hexabromocyclododecane (HBCD), and three commercial mixtures of polybrominated diphenyl ethers (PBDEs), which are known as decabromodiphenyl ether (DBDE), octabromodiphenyl ether (OBDE), and pentabromodiphenyl ether (pentaBDE). They are used as additive or reactive components in a variety of polymers, such as polystyrene foams, high-impact polystyrene, and epoxy resins [10]. BFRs are ubiquitously used as industrial materials worldwide. TBBPA accounted for approximately 76% of the BFRs consumed in Asia in 2001, and the amount used was approximately 90,000 tons [10]. BFRs are easily released into an environment due to deterioration or abrasion of the materials, but there is limited knowledge about their effects on health, particularly their effects on the immune systems of mammals [11–13]. To evaluate human health damage due to this environmental contaminant, the

* Corresponding author. Tel.: +81 982 23 5578; fax: +81 982 23 5684.
E-mail address: b2mk@phoenix.ac.jp (M. Kurokawa).

1567-5769/$ – see front matter © 2010 Elsevier B.V. All rights reserved.
doi:10.1016/j.intimp.2009.12.014

mechanism of action of BFRs on the immune system needs to be clarified.

In this study, the effects of DBDE, HBCD and TBBPA on host immunity were comparatively evaluated using the RSV infection mouse model.

2. Materials and methods

2.1. Mice

Female (4 weeks old) BALB/c mice were purchased from Kyudo Animal Laboratory (Kumamoto, Japan) and housed at 25 ± 2 °C. The mice were allowed free access to a conventional solid diet CRF-1 (Oriental Yeast Co., Chiba, Japan) and water and used in this experiment after 7 days acclimation. The animal experimentation guideline of the Kyushu University of Health and Welfare was followed in the animal studies.

2.2. Cells and virus

Human epidermoid carcinoma (HEp-2) cells (American Type Culture Collection CCL-23) were purchased from Dainippon Pharmaceutical (Osaka, Japan) and maintained in Eagle's minimum essential medium supplemented with heat-inactivated 10% fetal calf serum (FCS). The A2 strain of RSV was obtained from American Type Culture Collection (Rockville, MD) and grown in HEp-2 cell cultures. Viral titers of HEp-2 cells were measured by the plaque method, and expressed as plaque-forming units per milliliter (PFU/ml) [8].

2.3. BFRs

DBDE was purchased from Wako Pure Chemicals (Osaka, Japan). HBCD and TBBPA were purchased from Tokyo Kasei (Tokyo, Japan). They were mixed into a powder diet, which was soy-free to avoid the estrogen-like effect of soybeans, based on the formulation of the NIH-07 open-formula rodent diet [14] and produced by Oriental Yeast Co (Chiba, Japan).

2.4. Animal tests

Five-week-old female mice were fed a soy-free diet mixed with 1% DBDE, HBCD or TBBPA for 4 weeks. After treatment, these mice were fed CRF-1 and used for the following RSV infection test. Throughout the experiments, both chows and drinking water were given ad libitum.

The RSV infection test was performed as reported previously [9]. Briefly, 9-week-old female mice were infected intranasally with 1×10^6 or 1×10^5 PFU per 0.1 ml of the A2 strain of RSV under anesthesia. Mock-infected mice were also inoculated intranasally with 0.1 ml of phosphate-buffered saline (PBS) under anesthesia. On days 1, 3, 5 and 7 after infection, bronchoalveolar lavage fluid (BALF) was obtained from the mice under anesthesia by instilling of 1.0 ml of cold PBS into the lungs and aspirating it from the trachea using a tracheal cannula [15]. Ice-cold BALF was centrifuged at 100 × g at 4 °C for 10 min. After centrifugation, the supernatant was stored at −80 °C until to use. The cell pellet was suspended in PBS on ice and used as bronchoalveolar lavage (BAL) cells. For virus titration, the lungs were removed on day 5 post-infection, immediately frozen in liquid N_2, and stored at −80 °C. Frozen lung tissue was homogenized with cold quartz sand in a homogenizer, and viral titers in the supernatants of the homogenates were measured by a plaque assay [8]. The spleen was removed and minced by a scissor to obtain the cell suspension. A single cell suspension of spleen in ice-cold PBS was prepared by the filtration through a sterilized nylon-mesh.

2.5. Histological methods

For histological examination of the infected lungs, mock- or RSV-infected mice were sacrificed on day 5 post-infection, and lungs were removed and placed in buffered formalin for a minimum of 24 h. The tissue was then embedded in low-melting point paraffin, sectioned at a thickness of 5 μm, and stained with hematoxylin and eosin.

2.6. ELISA

Interleukin (IL)-1β, IL-4, IL-6, IL-10, interferon (IFN)-γ and tumor necrosis factor (TNF)-α levels in BALF were measured using specific ELISA kits (Ready-set-go, eBioscience Inc., San Diego, CA) according to the manufacturer's instructions. IL-12 levels in BALF were also measured using a specific kit (Ready-set-go, eBioscience Inc.) for IL-12 p70, without interference by p40 monomer or the related protein IL-23, according to the manufacturer's instructions. These products were tested and found to conform to all eBioscience Inc. quality control release specifications. The lower limits of detection sensitivity in the kits are 8 (pg/mL) for IL-1β, 4 (pg/mL) for IL-4, 4 (pg/mL) for IL-6, 8 (pg/mL) for IL-10, 15 (pg/mL) for IL-12 p70, 4 (pg/mL) for IFN-γ, and 8 (pg/mL) for TNF-α. The intra- and inter-assay coefficients of variation for these ELISA were less than 10%.

2.7. Flow cytometric analysis of BAL and spleen cells

Two-color analysis of BAL cells and spleen cells was performed using a FACS Calibur 3S flow cytometer (Becton Dickinson, Sunnyvale, CA). The following antibodies were used for phenotyping of murine cells: phycoerythrin (PE)-labeled hamster anti-CD3 (145-2C11), rat anti-CD8 (53.6), rat anti-CD11b (M1/70) and rat anti-CD49b (DX5) antibodies, fluorescein isothiocyanate (FITC)-labeled rat anti-CD4 (L3T4) and rat anti-CD25 (7D4) antibodies. All antibodies were purchased from BD Bioscience Pharmingen (San Diego, CA). Samples for analysis were prepared according to the manufacturer's instructions. Briefly, 0.05 ml of a single cell suspension (5×10^5 cells) in PBS was incubated with 0.02 ml of each PE-labeled antibody at 4 °C for 30 min. After incubation, the cells were washed with PBS and then incubated with 0.02 ml of each FITC-labeled antibody at 4 °C for 30 min. The cells were then washed as described above. After staining, at least 10,000 cells suspended in PBS on ice were analyzed by FACS. Finally, the data were analyzed with Cellquest software.

2.8. Statistical analysis

Comparisons of pulmonary viral titers and the levels of cytokines of the control and experimental groups were carried out using Student's *t*-test. A *P* value of 0.05 or less was considered to be significant.

3. Results

3.1. Effects of BFRs on RSV infection in mice

The effects of three BFRs on the severity of RSV infection in mice were investigated. Five-week-old female BALB/c mice were fed a diet containing 1% DBDE, HBCD, or TBBPA for 28 days. No loss of body weight at 28 day or decrease in food consumption during the treatment was detected in BFR-treated mice (Table 1). No particular toxicological sign, such as tremor, or abnormal behavior was observed in these mice either. Then, the mice were intranasally infected with

Table 1
Body weights and food consumption of DBDE-, HBCD- and TBBPA-treated mice.[a]

Index	Experiment 1			Experiment 2	
	Control	DBDE	HBCD	Control	TBBPA
Body weight (g)	20.8 ± 1.1	21.9 ± 1.2	21.2 ± 0.6	20.3 ± 1.1	19.6 ± 0.9
Food consumption (g/week)	25.7 ± 0.3	26.4 ± 0.5	26.8 ± 0.4	24.1 ± 4.1	25.1 ± 2.2

[a] Values represent mean ± standard deviation of 6–7 mice.

the A2 strain of RSV at 1×10^6 PFU. On day 5 after RSV infection, pulmonary viral titers were significantly ($P<0.001$) increased in TBBPA-treated mice compared with the control (Table 2). However, an obvious increase in the pulmonary viral titers was not observed in DBDE- or HBCD-treated mice. To confirm the effects of TBBPA on RSV infection, an additional group was instilled with a low titer (1×10^5 PFU) of RSV (Table 2). The pulmonary viral titers in low-titer TBBPA-treated mice were significantly ($P<0.05$) higher than those in control mice as well. Then, to investigate whether TBBPA directly promotes the growth of virus, the effect of TBBPA on the replication of RSV was tested in vitro using HEp-2 cell cultures, with the result that the compound did not affect the growth of RSV (data not shown). Thus, although BFRs did not show any apparent toxicity in mice in this study, TBBPA increased the RSV titers in the lung tissues of RSV-infected mice.

3.2. Effects of TBBPA on the development of pneumonia in RSV-infected mice

The effects of TBBPA ingestion on lung tissues of RSV-infected mice were analyzed histopathologically. While typical features of pneumonia such as infiltrations of lymphocytes and neutrophils due to RSV infection were observed on day 5 post-infection in mice treated with and without TBBPA (Fig. 1a, b), severely exacerbated pneumonia with expansion of the inflammation and hyperplasia of macrophages were found in the infected mice treated with TBBPA (Fig. 1b). In mock-infected mice, mild inflammation and congestion were observed in TBBPA-treated mice compared with the control (Fig. 1c, d). These results indicated that TBBPA caused mild immune injury in lung tissues and that the lesion was exacerbated to severe pneumonia by RSV infection in mice.

3.3. Effects of TBBPA on levels of cytokines in BALF from RSV-infected mice

To investigate the effects of TBBPA on the immune system, the levels of various cytokines in BALF induced by RSV infection in mice treated with TBBPA were measured by ELISA on day 1, 3, 5 and 7 post-infection (Table 3). The levels of IFN-γ, a representative marker of pneumonia due to RSV infection, in BALF from TBBPA-treated mice were significantly ($P<0.01$) increased and approximately 5.2-fold of the control on day 5 post-infection. IFN-γ could not be detected in BALF from mock-infected mice with or without TBBPA treatment (data not shown). On day 1 post-infection, the levels of both TNF-α and IL-6 in TBBPA-treated mice were significantly ($P<0.05$) increased to 5.8- and 2.6 times, respectively, of the control. No significant increase of IL-1β or IL-12 was found after TBBPA treatment. In contrast to these results, the levels of both IL-4 and IL-10, Th2 cytokines, were significantly ($P<0.05$) reduced on day 7 post-infection in BALF from TBBPA-treated mice compared with the control. Thus, TBBPA treatment enhanced production of TNF-α, IL-6 and IFN-γ but suppressed production of IL-4 and IL-10 in RSV-infected mice.

Table 2
Effects of treatment of DBDE, HBCD and TBBPA on pulmonary viral titers on day 5 post-infection in RSV-infected mice.[a]

Group/BFRs treatment	Pulmonary viral titers (PFU/ml)		
	Experiment 1	Experiment 2	Experiment 3
Control	14,833 ± 8,566	17,433 ± 3,670	526 ± 146
DBDE	19,111 ± 18,000	ND	ND
HBCD	13,875 ± 2,776	ND	ND
TBBPA	ND	34,967 ± 7742**	1630 ± 764*

*Statistically different from control at $P<0.05$ (Student's t-test).
**Statistically different from control at $P<0.001$ (Student's t-test).
[a] Values represent mean ± standard deviation of 6–7 mice. Mice were infected intranasally with 1×10^6 PFU of RSV in experiments 1 and 2, and with 1×10^5 PFU in experiment 3. ND, not determined.

3.4. Effect of TBBPA on cell populations in BAL and spleen cells in RSV-infected mice

To clarify the effects of TBBPA on immune responses in RSV-infected mice, the cell populations of BAL and spleen cells were analyzed on days 1 and 3 post-infection by flow cytometry (Table 4). There were no significant differences in the number of BAL cells in control and TBBPA-treated mice groups in RSV-infected mice (data not shown). On day 1 post-infection, CD11b+ (positive) cells, dendritic cells or macrophages, accounted for more than 90% of BAL cells, and a difference in the population ratios of the control and TBBPA-treated mice was not observed. However, the percentages of double-positive T cells (CD4+CD8+), immature T cells, were markedly increased in BAL cells from RSV-infected mice due to treatment with TBBPA on day 3 post-infection, although there was no difference the number of CD4+CD8+ cells in mock-infected mice. The percentages of CD49b+ cells, NK cells, in BAL cells on days 1 and 3 post-infection were not affected by treatment with TBBPA. Although TBBPA reduced the ratio of CD3+CD25+ cells, activated T cells, on day 1 post-infection, they were low overall in BALF from RSV-infected mice. To evaluate the effects of TBBPA treatment on systemic immunity, CD11b+ and CD4+CD8+ cells in spleens of mock- and RSV-infected mice were analyzed on day 3 post-infection, but no difference due to TBBPA treatment was observed in the treated mice.

4. Discussion

To evaluate the effects of three BFRs on the host immunity of mice, a murine RSV infection model was used in this study [8,9]. Although mice were fed a diet containing 1% BFR for 4 weeks, no toxicity was observed in the BFR-treated mice (Table 1). The dosage of BFRs based on the average food consumption and body weight was calculated at approximately 1700 mg/kg/day (Table 1). The dosage sounds very high, but these BFRs were reported to be non-toxic in mice at this dosage for this treatment period [16,17], and our results were consistent with the reports. However, a significant ($P<0.001$) increase of pulmonary viral titers was detected in TBBPA-treated mice compared with the control, but not in DBDE- or HBCD-treated mice (Table 2). Consequently, it was verified that TBBPA treatment enhanced RSV growth in the lungs of mice.

In a histopathological analysis, mild lesions of the lungs were detected after TBBPA treatment in mock-infected mice (Fig. 1). Moreover, the administration of TBBPA was shown clearly to increase virus titers in the lungs (Table 2) and exacerbate the pneumonia in RSV-infected mice. Previously, treatment with an immunosuppressive agent, cyclophosphamide, was shown to increase pulmonary viral titers and exacerbate the pneumonia in RSV-infected mice [5,8]. This suggests that immune conditions in the host contribute to pulmonary virus titers and exacerbation of pneumonia. Thus, TBBPA might induce a disorder of the immunity against RSV infection, resulting in the increase of virus titers and exacerbation of pneumonia.

To clarify the immune disorder due to TBBPA administration, cytokine productions induced by RSV infection were examined (Table 3). In TBBPA-treated mice, marked increases of IL-6 and TNF-α were observed on day 1 post-infection. It was reported that these cytokines increase immediately in the early phase after RSV infection [18,19]. On the other hand, productions of IL-1β and IL-12, which are produced mainly by macrophages and dendritic cells, were not affected by TBBPA. As reported previously [8,9], the levels of IFN-γ, a marker of pneumonia, increased maximally on day 5 post-infection in RSV-infected mice, and its production was enhanced in TBBPA-treated mice (Table 3). The increase of IFN-γ may be induced by the increased IL-6 and TNF-α. Thus, these irregular cytokine productions indicate

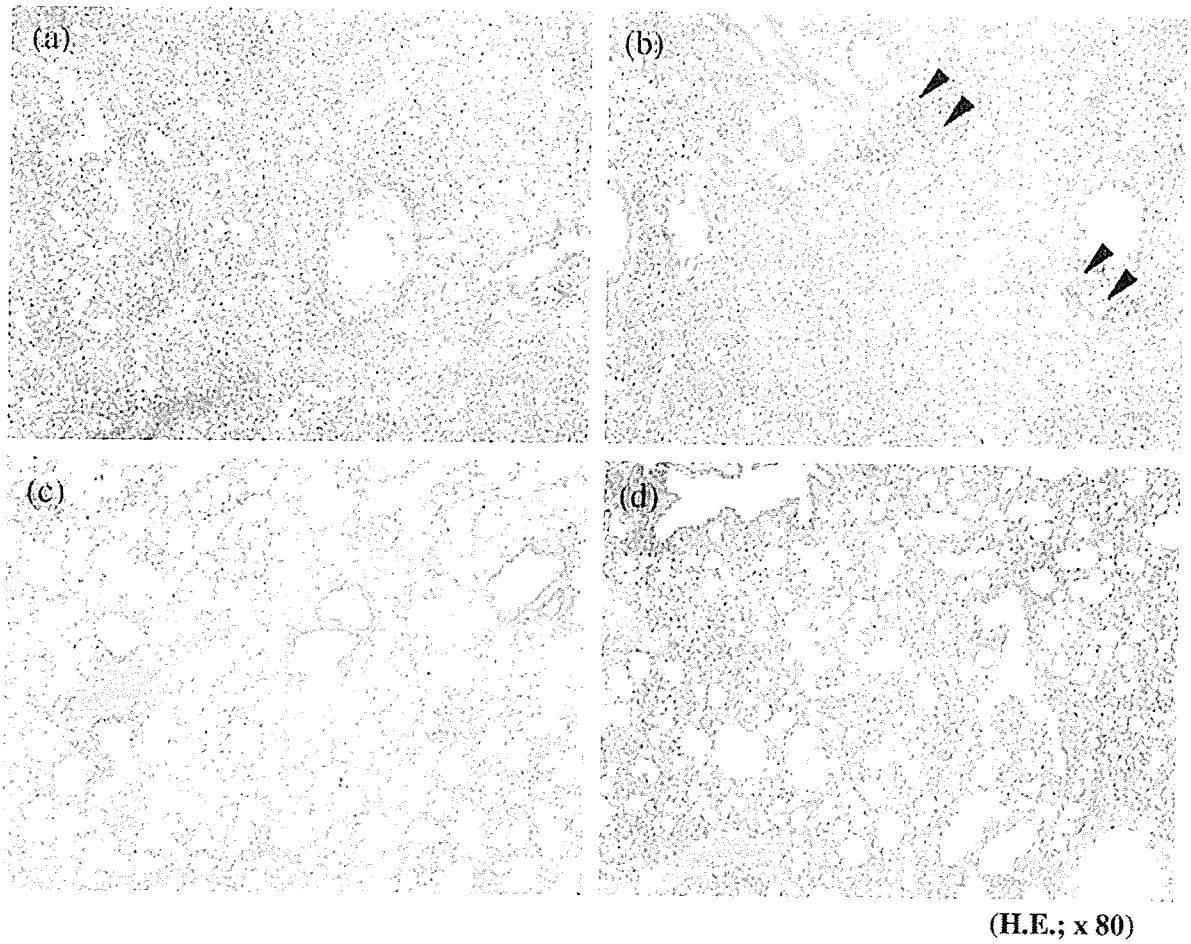

Fig. 1. Lungs of mice 5 days after mock or RSV infection. In this experiment, 4–5 mice per group were used, and representative data are shown. Arrowheads indicate macrophage hyperplasia. (a) Control mouse with RSV infection. (b) TBBPA-treated mouse with RSV infection. (c) Control mouse with mock infection. (d) TBBPA-treated mouse with mock infection. Hematoxylin and eosin stain.

that TBBPA caused disorder of the immune system in RSV-infected mice. Because the MAP kinases and protein kinase C were reported to be activated by TBBPA [20,21], disorder of the signal transduction system may be involved in the unusual production of the cytokines. On day 7 post-infection, IL-4 and IL-10, Th2 cytokines, were decreased in TBBPA-treated mice (Table 3). Studies for the development of a vaccine demonstrated that an imbalance of Th1/2 cytokines in the immune system is involved in the severity of RSV-induced disease [22]. Because TBBPA treatment strongly enhanced the production of

Table 3
Effects of TBBPA on cytokine concentration in BALF from RSV-infected mice.[a]

	Day 1 pi		Day 3 pi		Day 5 pi		Day 7 pi	
Cytokine	Control	TBBPA	Control	TBBPA	Control	TBBPA	Control	TBBPA
TNF-α	0.25 (0.17)	1.44* (0.74)	0.11 (0.02)	0.14 (0.03)	ND	ND	ND	ND
IL-1β	<0.04	0.05 (0.01)	ND	ND	ND	ND	ND	ND
IL-6	0.40 (0.14)	1.05*,# (0.06)	<0.02	<0.02	ND	ND	ND	ND
IL-12	0.11 (0.01)	0.15 (0.05)	0.15 (0.01)	0.18 (0.04)	ND	ND	ND	ND
IFN-γ	0.12 (0.02)	0.22 (0.07)	0.16 (0.02)	0.21 (0.07)	1.08 (0.86)	5.57*,# (2.82)	3.16 (2.66)	2.38 (0.99)
IL-4	ND	ND	<0.02	<0.02	0.04 (0.01)	0.03 (0.01)	0.06 (0.01)	0.04*,# (0.01)
IL-10	ND	ND	<0.08	<0.08	0.09 (0.02)	0.07 (0.02)	0.16 (0.02)	0.13# (0.01)

*Statistically different from control at $P<0.05$ (Student's t-test). **Statistically different from control at $P<0.01$ (Student's t-test).

[a] Concentration (ng/ml) of each cytokine in BALF from RSV-infected mice treated with or without 1% TBBPA was measured by ELISA for each specific cytokine. Data represents mean values of 5–6 mice. Numbers in parentheses indicate standard deviation. ND, not determined.

Table 4
Effects of TBBPA on subpopulations in BAL and spleen cells of RSV-infected mice.

	% of total cell populations[a]					
	BAL cells				Spleen cells	
	Day 1 pi		Day 3 pi		Day 3 pi	
Subpopulation	Control	TBBPA	Control	TBBPA	Control	TBBPA
RSV-infected						
CD11b	91.2	92.5	24.1	24.1	10.5	6.7
CD49b	23.1	30.5	25.9	23.7	ND	ND
CD4CD8	5.3	4.0	16.0	29.1	0.1	0.1
CD3CD25	2.8	0.8	2.8	2.2	ND	ND
Mock-infected						
CD11b	ND	ND	ND	ND	6.8	7.5
CD4CD8	ND	ND	23.5	19.6	ND	ND

Spleen cells were obtained from a representative mouse in each group. ND, not determined; pi, post-infection.

[a] BAL cells were collected from 6 mice in each group on day 1 or day 3 post-infection and pooled by group.

Th1 cytokines such as IFN-γ, Th2 cytokines might be suppressed reciprocally in TBBPA-treated mice with RSV infection.

To clarify the disorder in immune cell populations due to TBBPA administration, FACS analysis was performed on BAL cells (Table 4). Initially, it was speculated that macrophages and/or dendritic cells were affected in TBBPA-treated mice, because they mainly work in the early phase of RSV infection [19] and produce IL-6 and TNF-α (Table 3). However, the percentages of CD11b+ cells did not differ in control and TBBPA-treated mice. The numbers of CD11b molecules per cell as monitored by the intensity of fluorescence did not differ in the groups either (data not shown). TBBPA might have induced a qualitative change in immune cells that worked in the early phase of RSV infection. Pullen et al. reported that activated T cells, CD3+CD25+ cells, were damaged by TBBPA in murine spleen cell cultures in vitro [12]. However, the percentages of CD3+CD25+ cell populations in BAL cells were not clearly changed by TBBPA treatment in this study. NK cells (CD49b+), which work to eliminate RSV as an early induced immune response [23], were not affected either. Only the percentages of double-positive T (CD4+CD8+) cell populations were affected by TBBPA treatment in this study. Partial inhibition of the maturation of T cells due to TBBPA may result in an increase of viral titers (Table 2). Thus, TBBPA affected not only the quality of immune cells but also the maturation of T cells in local immunity in mice.

RSV infection is an important infectious disease in the field of pediatrics because clinically severe RSV infection has been seen primarily in young children with naïve immune systems and/or genetic dispositions [3]. It was reported that RSV infection in early life was related to the risk of asthma in childhood [24,25]. Therefore, the exacerbation of RSV infection demonstrated in this study needs to be avoided in children. Moreover, developmental exposure to BFRs threatens to cause more severe disorder of the host immunity in RSV-infected mouse pups because DBDE was reported to show immunotoxicity in RSV-infected offspring mice after perinatal exposure [9], although the compound did not have that affect in this study. From the view point of the health of mothers and children, it is important to reduce contamination of the environment by TBBPA.

Acknowledgments

We thank Dr. Masaya Takeuchi (Sapporo General Pathology Laboratory, Sapporo, Japan) who stained and evaluated lung tissues. We also thank Katherine Ono for editing the manuscript. This work was supported by Health and Labour Sciences Research Grants (Research on Risk of Chemical Substances) from the Ministry of Health, Labour and Welfare of Japan and partly by Grant-in-Aid for Scientific Research (No. 20590131) and for Young Scientists (No. 20790430) from the Japan Society for the Promotion of Science.

References

[1] MacDonald NE, Hall CB, Suffin SC, Alexson C, Harris PJ, Manning JA. Respiratory syncytial viral infection in infants with congenital heart disease. N Engl J Med 1982;307:397–400.
[2] Collins PL, Chanock RM, Murphy BR. Respiratory syncytial virus. In: Knipe DM, Howley PM, editors. Fields virology. Philadelphia, Pa: Lippincott Williams&Wilkins; 2001. p. 1443–85.
[3] Holberg CJ, Wright AL, Martinez FD, Ray CG, Taussig LM, Lebowitz MD. Risk factors for respiratory syncytial virus-associated lower respiratory illnesses in the first year of life. Am J Epidemiol 1991;133:1135–51.
[4] Morales F, Calder MA, Inglis JM, Murdoch PS, Williamson J. A study of respiratory infections in the elderly to assess the role of respiratory syncytial virus. J Infect 1983;7:236–47.
[5] Sudo K, Watanabe W, Mori S, Konno K, Shigeta S, Yokota T. Mouse model of respiratory syncytial virus infection to evaluate antiviral activity in vivo. Antivir Chem Chemother 1999;10:135–9.
[6] Graham BS, Perkins MD, Wright PF, Karzon DT. Primary respiratory syncytial virus infection in mice. J Med Virol 1988;26:153–62.
[7] Wyde PR, Ambrose MW, Meyer HL, Gilbert BE. Toxicity and antiviral activity of LY253963 against respiratory syncytial and parainfluenza type 3 viruses in tissue culture and in cotton rats. Antivir Res 1990;14:237–47.
[8] Watanabe W, Shimizu T, Hino A, Kurokawa M. A new assay system for evaluation of developmental immunotoxicity of chemical compounds using respiratory syncytial virus infection to offspring mice. Environ Toxicol Pharmacol 2008;25:69–74.
[9] Watanabe W, Shimizu T, Hino A, Kurokawa M. Effects of decabrominated diphenyl ether (DBDE) on developmental immunotoxicity in offspring mice. Environ Toxicol Pharmacol 2008;26:315–9.
[10] Birnbaum LS, Staskal DF. Brominated flame retardants: cause for concern? Environ Health Perspect 2004;112:9–17.
[11] Lundgren M, Darnerud PO, Blomberg J, Friman G, Ilbäck NG. Polybrominated diphenyl ether exposure suppresses cytokines important in the defence to coxsackievirus B3 infection in mice. Toxicol Lett 2009;184:107–13.
[12] Pullen S, Boecker R, Tiegs G. The flame retardants tetrabromobisphenol A and tetrabromobisphenol A-bisallyether suppress the induction of interleukin-2 receptor alpha chain (CD25) in murine splenocytes. Toxicology 2003;184:11–22.
[13] Teshima R, Nakamura R, Nakamura R, Hachisuka A, Sawada J, Shibutani M. Effects of exposure to decabromodiphenyl ether on the development of the immune system in rats. J Health Sci 2008;54:382–9.
[14] Masutomi N, Shibutani M, Takagi H, Ueyama C, Hirose M. Dietary influence on the impact of ethinylestradiol-induced alterations in the endocrine/reproductive system with perinatal maternal exposure. Reprod Toxicol 2004;18:23–33.
[15] Kurokawa M, Tsurita M, Brown J, Fukuda Y, Shiraki K. Effect of interleukin-12 level augmented by Kakkon-to, a herbal medicine, on the early stage of influenza infection in mice. Antivir Res 2002;56:183–8.
[16] National Toxicology Program. NTP toxicology and carcinogenesis studies of decabromodiphenyl oxide (CAS No. 1163-19-5) in F344/N rats and B6C3F1 mice (feed studies). Natl Toxicol Program Tech Rep Ser 1986;309:1–242.
[17] Tada Y, Fujitani T, Yano N, Takahashi H, Yuzawa K, Ando H, et al. Effects of tetrabromobisphenol A, brominated flame retardant, in ICR mice after prenatal and postnatal exposure. Food Chem Toxicol 2006;44:1408–13.
[18] Janeway CA, Travers P, Walport M, Shlomchik MJ. Innate immunity. immunobiology: the immune system in health and disease. 5th ed. New York, NY: Garland Publishing; 2001. p. 35–91.
[19] Neuzil KM, Tang YW, Graham BS. Protective role of TNF-alpha in respiratory syncytial virus infection in vitro and in vivo. Am J Med Sci 1996;311:201–4.
[20] Canesi L, Lorusso LC, Ciacci C, Betti M, Gallo G. Effects of the brominated flame retardant tetrabromobisphenol-A (TBBPA) on cell signaling and function of *Mytilus* hemocytes: involvement of MAP kinases and protein kinase C. Aquat Toxicol 2005;75:277–87.
[21] Reistad T, Mariussen E. A commercial mixture of the brominated flame retardant pentabrominated diphenyl ether (DE-71) induces respiratory burst in human neutrophil granulocytes in vitro. Toxicol Sci 2005;87:57–65.
[22] Waris ME, Tsou C, Erdman DD, Zaki SR, Anderson LJ. Respiratory syncytial virus infection in BALB/c mice previously immunized with formalin-inactivated virus induces enhanced pulmonary inflammatory response with a predominant Th2-like cytokine pattern. J Virol 1996;70:2852–60.
[23] Hussell T, Openshaw PJ. Intracellular IFN-gamma expression in natural killer cells precedes lung CD8+ T cell recruitment during respiratory syncytial virus infection. J Gen Virol 1998;7:2593–601.
[24] Sigurs N, Gustafsson PM, Bjarnason R, Lundberg F, Schimdt S, Sigurbergsson F, et al. Severe respiratory syncytial virus bromchiolitis in infancy and asthma and allergy at age 13. Am J Respir Crit Care Med 2005;171:137–41.
[25] Stein RT, Sherrill D, Morgan WJ, Holberg CJ, Halonen M, Taussig LM, et al. Respiratory syncytial virus in early life and risk of wheeze and allergy by age 13 years. Lancet 1999;354:541–5.